Mathematical Modelling and Analysis
Volume 9 Number 4, 2004, pages 253–266
 ISSN 1392-6292

IMPLICIT NUMERICAL ALGORITHM FOR THE SOLUTION OF PHASE TRANSITION PROBLEMS IN MULTI-COMPONENT ALLOYS

O.V. CHTCHERITSA, O.S. MAZHOROVA and YU.P. POPOV

Keldysh Institute of Applied Mathematics, Russia Academy of Science

Miusskaya Sq.4, 125047, Moscow, Russia

E-mail: magor@keldysh.ru

Received June 16, 2004; revised November 3, 2004

Abstract. New finite difference method for numerical study of phase transition process in multi-component alloys is proposed. The algorithm is based on conservative fully implicit scheme and the simultaneous determination of concentration distribution in solid and liquid phases, and the interface position. The numerical procedure appears to be unconditionally stable. It is compared with a commonly used technique, which determines concentration distribution and interface position (growth rate) consequently.

Key words: Computer simulation, phase transition, finite difference scheme, modelling

1. Introduction

In resent years computer simulation for mass transfer in the systems with phase transition becomes one of the most challenging problems in computational fluid dynamics. The research in this field is encouraged by the important role of phase change processes in modern technology, especially in crystal growth. Modelling activities accompany any development of a new crystal growth facility, as well as improvement or up-scaling of the existing setup [12]. A lot of advanced numerical algorithms have been introduced for computer simulation of solid/liquid phase transition [15]. Most of them are based on classical Stefan problem and deal with the process in pure materials or dilute alloys, and very few consider the solidification in non-dilute multi-component media. The last problem is more sophisticated because in such processes the phase transition temperature depends on the composition

of the liquid and solid phases. That distinguishes it from the classical Stefan problem where the transition temperature is constant.

Here we propose the numerical procedure for simulation of solid/liquid phase change in ternary solution. The problem is considered in 1D approach. The mathematical model takes into account diffusion in the solid and the liquid phases and evolution of the phase volumes due to the interface motion. There are mass balance conditions and phase diagram of the system, which connects solution concentration to the composition of the solid phase and temperature, imposed at the solid-liquid interface. The model is self-consistent. It allows to predict both growth and dissolution processes as well as species distribution in the solid phase, that is of primary importance for crystal growers.

Special efforts are required to design stable and reliable algorithm for solving such problems, no matter one dimensional. The main difficulties are associated with strong coupling between the composition of the liquid and solid phases and with wide range of time scales introduced by interface motion, diffusion in the crystal and in the solution.

We describe the proposed algorithm considering the epitaxial growth of monocrystal layers as an example. The numerical procedure developed in this study is suitable for the simulation of general phase transition processes in ternary alloys.

2. Mathematical Model

The basic principle of liquid phase epitaxy (LPE) is similar to the growth of salt crystals from a saturated saline solution [2, 6, 16]. A solution of the components A and B in liquid C is brought into contact with a substrate AC or $A_xB_{1-x}C$. If the solution is slightly supersaturated, components A and B precipitate out of the solution onto the substrate, providing crystal growth process. Supersaturation is usually maintained by gradual cooling of the system. The numerical study for LPE process of $A_xB_{1-x}C$ is based on the following assumptions [5, 6]:

a) the growth takes place under quasi–equilibrium conditions;

b) at the solid/liquid interface the composition of the two phases are related by the phase diagram of the system;

c) due to high thermal conductivity of the materials and slow cooling, the temperature distribution is uniform throughout the system and changes in time according to a prescribed rule.

2.1. Governing equations

The system is described by the concentration distribution of the solid and liquid phases and by the interface position.

The domain $\widetilde{\mathrm{D}}_1 = \{\tilde{\mathrm{x}}_1 \le \tilde{\mathrm{x}} \le \tilde{\mathrm{x}}_2\}$, denoted as the solid phase, consists of the substrate and epitaxial layers. $\widetilde{\mathrm{D}}_2 = \{\tilde{\mathrm{x}}_2 \le \tilde{\mathrm{x}} \le \tilde{\mathrm{x}}_3\}$ corresponds to the liquid phase, $\tilde{\mathrm{x}}_2(\tilde{\mathrm{t}})$ is time-dependent coordinate of solid/liquid interface (see Fig. 1).

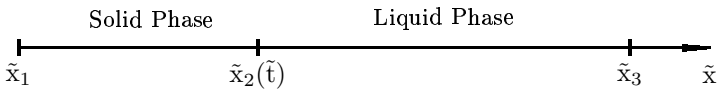

Figure 1. Computational domain.

We consider the solidification of a ternary alloy, where components A, B are dissolved in the melted C. There are three compositional variables that define the composition of the liquid phase: $x^{(A)}$ and $x^{(B)}$ and $x^{(C)}$ which must satisfy the equality

$$x^{(A)} + x^{(B)} + x^{(C)} = 1.$$

Here $x^{(A)}$, $x^{(B)}$ and $x^{(C)}$ are respectively the mole fractions of components A, B and C in the liquid. It means that only two variables, let it be $x^{(A)}$, $x^{(B)}$, are independent.

In the solid phase, only one compositional variable x is needed to describe the composition, since

$$x^{s(A)} = 0.5x, \quad x^{s(B)} = 0.5(1-x), \quad x^{s(C)} = 0.5\,. \tag{2.1}$$

Here $x^{s(A)}$, $x^{s(B)}$ and $x^{s(C)}$ are the mole fractions of components A, B and C in the solid, x is the mole fraction of AC in $A_xB_{1-x}C$.

Mass transfer in bulk phases is determined by diffusion

$$\begin{aligned} &\frac{\partial c^{s(A)}}{\partial \tilde{t}} = D^{s(A)} \frac{\partial^2 c^{s(A)}}{\partial \tilde{x}^2}, && \tilde{x}_1 < \tilde{x} < \tilde{x}_2(\tilde{t}) \\ &\frac{\partial c^{l(j)}}{\partial \tilde{t}} = D^{l(j)} \frac{\partial^2 c^{l(j)}}{\partial \tilde{x}^2}, && \tilde{x}_2(\tilde{t}) < \tilde{x} < \tilde{x}_3, \qquad j = A,\, B, \end{aligned} \tag{2.2}$$

where $\tilde{x}$ is Cartesian coordinate, $\tilde{t}$ is the time, $D^{s(j)}$ and $D^{l(j)}$ are the diffusion coefficients of the component j in the solid and the liquid phases, $c^{s(j)}$ and $c^{l(j)}$ are the volume concentrations of the corresponding component in the solid and liquid phases respectively. Concentration of the component B in the solid phase is found from condition (2.1).

Boundary conditions at $\tilde{x} = \tilde{x}_1$ and $\tilde{x} = \tilde{x}_3$ are given as follows [1]:

$$\begin{aligned} &\frac{\partial c^{s(A)}}{\partial \tilde{x}} = 0, && \tilde{x} = \tilde{x}_1 \\ &\frac{\partial c^{l(j)}}{\partial \tilde{x}} = 0, && \tilde{x} = \tilde{x}_3,\ j = A,\, B. \end{aligned} \tag{2.3}$$

[1] In the sequel all parameters related to the solid phase will be referred with subscript "s". Parameters without subscripts relate to the liquid phase.

2.2. Solid-liquid interface conditions

The conditions at the interface represent the mass balance and phase equilibrium between two phases.

1. **Mass balance**:

$$D^{s(j)}\frac{\partial c^{s(j)}}{\partial \tilde{\mathrm{x}}}\bigg|_{\tilde{\mathrm{x}}_2(\tilde{\mathrm{t}})-0} - D^{l(j)}\frac{\partial c^{l(j)}}{\partial \tilde{\mathrm{x}}}\bigg|_{\tilde{\mathrm{x}}_2(\tilde{\mathrm{t}})+0} = -v_{ph}(c^{s(j)} - c^{l(j)}), \quad j = A,\, B, \quad \tilde{\mathrm{x}} = \tilde{\mathrm{x}}_2(\tilde{\mathrm{t}}), \tag{2.4}$$

   where $v_{ph} = \dot{\tilde{\mathrm{x}}}_2(\tilde{\mathrm{t}})$ is the interface rate.

2. **Phase diagram.** Composition of the two phases at the solid/liquid is related by phase diagram of the system, that can be written in the form [4]:

$$\begin{aligned} x^s_{AC} &= 4\gamma_A\, x^{(A)}\, x^{(C)}\, exp\left(\frac{\Delta H^{melt}_{AC}}{R\,T^{melt}_{AC}}\,\frac{T^{melt}_{AC} - T}{T}\right), \\ x^s_{BC} &= 4\gamma_B\, x^{(B)}\, x^{(C)}\, exp\left(\frac{\Delta H^{melt}_{BC}}{R\,T^{melt}_{BC}}\,\frac{T^{melt}_{BC} - T}{T}\right). \end{aligned} \tag{2.5}$$

   Here T is the temperature, R is the universal gas constant, ΔH^{melt}_{AC}, ΔH^{melt}_{BC} are the entropies of fusion, T^{melt}_{AC}, T^{melt}_{BC} are the melting points, γ_j $(j = A,\, B)$ are the polynomial expressions. The coefficients have been determined by the least – squares fitting of the available experiment data [4, 5].

In order to obtain the equation that is used in the simulation, x^s_{AC} and x^s_{BC} from (2.5) are substituted into (2.1):

$$x^{(A)} + k\, x^{(B)} = \frac{\eta}{1 - x^{(A)} - x^{(B)}}\,, \tag{2.6}$$

where

$$k = \frac{\gamma_B}{\gamma_A}\,\frac{exp\left(\dfrac{\Delta H^{melt}_{BC}}{R\,T^{melt}_{BC}}\,\dfrac{T^{melt}_{BC} - T}{T}\right)}{exp\left(\dfrac{\Delta H^{melt}_{AC}}{R\,T^{melt}_{AC}}\,\dfrac{T^{melt}_{AC} - T}{T}\right)}, \quad \eta = \frac{1}{4\,\gamma_A\, exp\left(\dfrac{\Delta H^{melt}_{AC}}{R\,T^{melt}_{AC}}\,\dfrac{T^{melt}_{AC} - T}{T}\right)}.$$

We rewrite (2.5), (2.6) in volume units. The concrete form of the phase diagram is not important for the further statement, so it is represented as

$$\begin{aligned} &\mathcal{F}(c^{(A)}, c^{(B)}) = 0, \\ &c^{s(j)} = f(c^{(A)}, c^{(B)}, T) \quad j = A,\, B, \quad \tilde{\mathrm{x}} = \tilde{\mathrm{x}}_2(\tilde{\mathrm{t}}) \end{aligned} \tag{2.7}$$

It should be noted, that transition from mole fraction to volume units is a nonlinear transformation.

3. Numerical Method

3.1. Coordinate transformation

To handle evolution of the solid/liquid interface, we map the moving boundary problem (2.2) – (2.4), (2.7) to the new coordinate system (see Fig. 2). The reference frame moves with the solid – liquid interface at the velocity υ_{ph}, i.e. in the new coordinate system the interface is fixed.

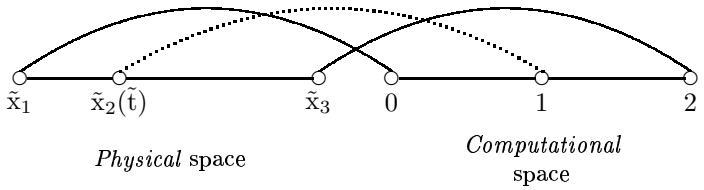

Figure 2. Coordinate transformation.

Coordinate transformation from the physical space $(\tilde{x}, \tilde{t})$ into the space of computational variables (x, t) reads:

$$\tilde{t} = t, \quad \tilde{x} = \varphi(x,t) = \begin{cases} \tilde{x}_1 + x\, l^s, & 0 \le x \le 1, \\ \tilde{x}_2 + (x-1)\, l^l, & 1 \le x \le 2, \end{cases}$$

l^s, l^l are widths of solid and liquid phases respectively. In the new coordinate system the interface is located at the point $x = 1$.

The governing equations in the *solid phase* $(0 \le x < 1)$ take the following form [1]:

$$\begin{cases} l^s \dfrac{\partial c^{s(A)}}{\partial t} - \varphi_t \dfrac{\partial c^{s(A)}}{\partial x} = \dfrac{\partial}{\partial \mathrm{x}} \left(\dfrac{D^{s(A)}}{l^s} \dfrac{\partial c^{s(A)}}{\partial x} \right), \\ (a_A + a_C) c^{s(A)} + (a_B + a_C) c^{s(B)} = \rho^s \,, \\ \left. \dfrac{\partial c^{s(A)}}{\partial x} \right|_{x=0} = 0 \,. \end{cases} \tag{3.1}$$

The second equation in (3.1) was obtained from condition (2.1) written in the form

$$x^{s(A)} + x^{s(B)} = \frac{1}{2}$$

and translated into volume units. Here ρ^s is the density of the solid, a_A, a_B and a_C are atomic weights of component A, B and C respectively.

Equations in the *liquid phase* $(1 < \mathrm{x} \le 2)$ are given as:

$$\begin{cases} l^l \dfrac{\partial c^{l(j)}}{\partial t} - \varphi_t \dfrac{\partial c^{l(j)}}{\partial x} = \dfrac{\partial}{\partial \mathrm{x}} \left(\dfrac{D^{l(j)}}{l^l} \dfrac{\partial c^{l(j)}}{\partial x} \right), \quad j = A,\, B\,, \\ \left. \dfrac{\partial c^{(j)}}{\partial x} \right|_{x=2} = 0, \qquad j = A,\, B\,. \end{cases} \tag{3.2}$$

Phase transition interface equations are given at $x = 1$:

$$\begin{cases} \left. \dfrac{D^{s(A)}}{l^s} \dfrac{\partial c^{s(A)}}{\partial x} \right|_{x=1-0} - \left. \dfrac{D^{l(A)}}{l^l} \dfrac{\partial c^{l(A)}}{\partial x} \right|_{\mathrm{x}=1+0} = -\upsilon_{ph} (c^{s(A)} - c^{l(A)})\,, \\ \left. \dfrac{D^{s(B)}}{l^s} \dfrac{\partial c^{s(B)}}{\partial x} \right|_{x=1-0} - \left. \dfrac{D^{l(B)}}{l^l} \dfrac{\partial c^{l(B)}}{\partial x} \right|_{\mathrm{x}=1+0} = -\upsilon_{ph} (c^{s(B)} - c^{l(B)})\,, \\ \mathcal{F}(c^{(A)}, c^{(B)}) = 0,\; c^{s(j)} = f(c^{(A)}, c^{(B)}, T), \quad j = A,\, B\,. \end{cases} \tag{3.3}$$

The transformed equations contain several additional terms and coefficients are not found in the generic conservation equations. The terms actually depend on interface rate υ_{ph}. They contribute to each equation in the system (3.1) – (3.3) emphasizing the coupling between the processes in the solid phase, fluid and at the interface.

3.2. Finite difference scheme

The numerical procedure for the solution of equations (3.1) – (3.3) is based on the conservative and implicit finite difference scheme that is obtained in new coordinate system by the control volume method [14].

Unknown functions $c^{s(A)}$, $c^{s(B)}$, υ_{ph}, $c^{(A)}$, $c^{(B)}$ are computed at the grid nodes, while φ, l^s, l^l, D^s, D^l are calculated at the center of the grid cells. Coefficients, which correspond to the coordinate system transformation and depend on the interface movement rate υ_{ph}, are treated in an implicit way. Additional transport terms are approximated by the second–order central difference. Schemes with central difference provide reliable results if mesh size h satisfies the stability condition $h < \dfrac{2D^{(s/l)}}{\upsilon_{ph}}$ [7, 8, 9]. So we use this condition to choose the step in the solid and liquid phases. Grid nodes are numbered from $-N_1$ to N_2 and the solid/liquid interface corresponds to grid node number 0.

The finite difference scheme can be written as[2]:

[2] Subscript indicates the number of a considered grid node, variables with a hat correspond to the advanced time level.

$$\widehat{l}^s\,\frac{h_{i-\frac12}}{2}(\hat{c}_i^{s(A)}-c_i^{s(A)})+\widehat{l}^s\,\frac{h_{i+\frac12}}{2}(\hat{c}_i^{s(A)}-c_i^{s(A)})$$
$$-\tau\left[\left.\frac{\widehat{\varphi}_t}{2}\right|_{\mathrm{x}_{i-\frac12}}(\hat{c}_i^{s(A)}-\hat{c}_{i-1}^{s(A)})+\left.\frac{\widehat{\varphi}_t}{2}\right|_{\mathrm{x}_{i+\frac12}}(\hat{c}_{i+1}^{s(A)}-\hat{c}_i^{s(A)})\right] \tag{3.4}$$
$$=\tau\left[\frac{D^{s(A)}}{\widehat{l}^s}\frac{\hat{c}_{i+1}^{s(A)}-\hat{c}_i^{s(A)}}{h_{i+\frac12}}-\frac{D^{s(A)}}{\widehat{l}^s}\frac{\hat{c}_0^{s(A)}-\hat{c}_{i-1}^{s(A)}}{h_{i-\frac12}}\right],\quad -N_1\le i<0\,,$$

$$(a_A+a_C)c_i^{s(A)}+(a_B+a_C)c_i^{s(B)}=\rho^s,\quad -N_1\le i<0\,, \tag{3.5}$$

$$\widehat{l}^s\frac{h_{-\frac12}}{2}(\hat{c}_0^{s(j)}-c_0^{s(j)})+\widehat{l}^l\frac{h_{\frac12}}{2}(\hat{c}_0^{l(j)}-c_0^{l(j)})$$
$$-\tau\left[\left.\frac{\widehat{\varphi}_t}{2}\right|_{x_{-\frac12}}(\hat{c}_0^{s(j)}-\hat{c}_{-1}^{s(j)})+\left.\frac{\widehat{\varphi}_t}{2}\right|_{x_{\frac12}}(\hat{c}_1^{l(j)}-\hat{c}_0^{l(j)})\right] \tag{3.6}$$
$$=\tau\left[-(\hat{c}_0^{s(j)}-\hat{c}_0^{l(j)})\widehat{v}_{ph}+\frac{D^{l(j)}}{\widehat{l}^l}\frac{\hat{c}_1^{l(j)}-\hat{c}_0^{l(j)}}{h_{\frac12}}-\frac{D^{s(j)}}{\widehat{l}^s}\frac{\hat{c}_0^{s(j)}-\hat{c}_{-1}^{s(j)}}{h_{-\frac12}}\right],\ j=A,\,B\,,$$

$$\mathcal{F}(\hat{c}_0^{(A)},\hat{c}_0^{(B)})=0,\ \ \hat{c}_0^{s(j)}=f(\hat{c}_0^{(A)},\hat{c}_0^{(B)},T),\quad j=A,\,B, \tag{3.7}$$

$$\widehat{l}^l\,\frac{h_{i-\frac12}}{2}(\hat{c}_i^{l(j)}-c_i^{l(j)})+\widehat{l}^l\,\frac{h_{i+\frac12}}{2}(\hat{c}_i^{l(j)}-c_i^{l(j)})$$
$$-\tau\left[\left.\frac{\widehat{\varphi}_t}{2}\right|_{x_{i-\frac12}}(\hat{c}_i^{l(j)}-\hat{c}_{i-1}^{l(j)})+\left.\frac{\widehat{\varphi}_t}{2}\right|_{x_{i+\frac12}}(\hat{c}_{i+1}^{l(j)}-\hat{c}_i^{l(j)})\right] \tag{3.8}$$
$$=\tau\left[\frac{D^{l(j)}}{\widehat{l}^l}\frac{\hat{c}_{i+1}^{l(j)}-\hat{c}_i^{l(j)}}{h_{i+\frac12}}-\frac{D^{l(j)}}{\widehat{l}^l}\frac{\hat{c}_0^{l(j)}-\hat{c}_{i-1}^{l(j)}}{h_{i-\frac12}}\right],\quad 0<i\le N_2,\ j=A,\,B,$$

where $x_{i-1/2}$ is the center of the cell $[x_{i-1},x_i]$, $h_{i-1/2}=x_i-x_{i-1}$. The approximation of diffusion fluxes is of second order accuracy in space and first order accuracy in time.

The system of nonlinear algebraic equations (3.4) – (3.8) is solved by the Newton method [14]. Let's write the full system in the operator notations:

$$\mathbf{F}(\zeta)=0, \tag{3.9}$$

here $\zeta=(\hat{c}_{-N_1}^{s(A)},\,\hat{c}_{-N_1}^{s(B)},\,\hat{c}_{-N_1+1}^{s(A)},...,\,\hat{c}_0^{s(A)},\,\hat{c}_0^{s(B)},\hat{v}_{ph},\,\hat{c}_0^{(A)},\,\hat{c}_0^{(B)},\,\hat{c}_1^{(A)},...,\,\hat{c}_{N_2}^{(B)})^T$. The iterative process for the solution of (3.9) is determined as follows:

$$\mathbf{F}'(\overset{(k)}{\zeta})\delta\zeta+\mathbf{F}(\overset{(k)}{\zeta})=0,$$

where $\mathbf{F}'$ is the Jacobian matrix, $\delta\zeta=\overset{(k+1)}{\zeta}-\overset{(k)}{\zeta}$, k is the Newton iteration counter. The solution from the previous time level is used as a starting estimate for the iteration.

At each Newton iteration we have the system of linear equations with respect to unknown vector $\delta\zeta$, the components of which are increments of concentrations of all species

$$\delta c_i^{s(j)}, \;\; i = -N_1, ..., 0, \quad \delta c_i^{l(j)}, \;\; i = 0, ..., N_2, \;\; j = A, \, B$$

and interface rate δv_{ph}. The Jacobian matrix is defined as:

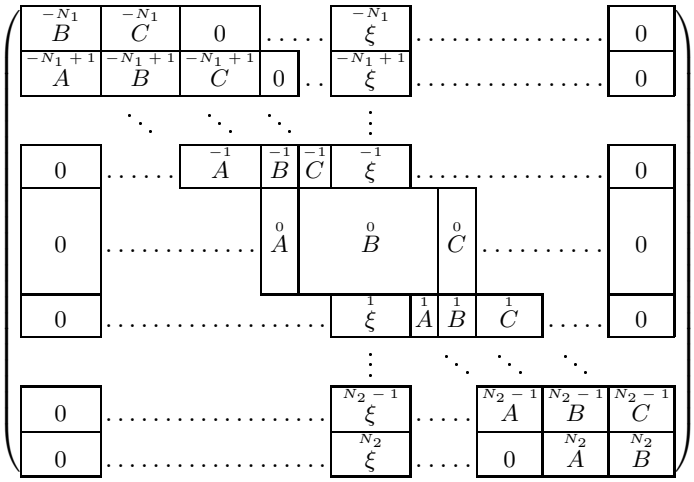

The blocks in this matrix have the following structure:

$$\overset{i}{A}, \overset{i}{C} = \begin{cases} \begin{pmatrix} * & 0 \\ 0 & 0 \end{pmatrix}, & -N_1 \le i < 0, \\ \\ \begin{pmatrix} * & 0 \\ 0 & * \end{pmatrix}, & 0 < i \le N_2, \end{cases} \qquad \overset{i}{B} = \begin{cases} \begin{pmatrix} * & 0 \\ * & * \end{pmatrix}, & -N_1 \le i < 0, \\ \\ \begin{pmatrix} * & 0 \\ 0 & * \end{pmatrix}, & 0 < i \le N_2, \end{cases}$$

$$\overset{i}{\xi} = \begin{cases} \begin{pmatrix} * \\ 0 \end{pmatrix}, & -N_1 \le i < 0\,, \\ \\ \begin{pmatrix} * \\ * \end{pmatrix}, & 0 < i \le N_2\,. \end{cases}$$

$\overset{0}{A}$ and $\overset{0}{C}$ are 2×5 blocks, $\overset{0}{B}$ is 5×5 block:

$$\overset{0}{A}, \overset{0}{C} = \begin{pmatrix} * & 0 \\ 0 & * \\ 0 & 0 \\ 0 & 0 \\ 0 & 0 \end{pmatrix}, \quad \overset{0}{B} = \begin{pmatrix} * & 0 & * & * & 0 \\ 0 & * & * & 0 & * \\ 0 & 0 & 0 & * & * \\ * & * & 0 & * & * \\ * & * & 0 & * & * \end{pmatrix}.$$

The full column in the center of the matrix corresponds to the unknown interface rate.

In order to obtain the solution of the corresponding linear system the modified Thomas algorithm is used [13]. We represent $\delta c_i^{s(A)}$, $i = -N_1, \ldots, 0$, $\delta c_i^{(j)}$, $j = A, B$, $i = 0, \ldots, N_2$, δv_{ph} in the following form

$$\delta c_i^{s(A)} = \alpha_{i+1}^s \delta c_{i+1}^{s(\mathbf{A})} + \beta_{i+1}^s + \gamma_{i+1}^s \delta v_{ph}, \quad -N_1 \le i \le -1,$$
$$\delta c_i^{(j)} = \alpha_{i-1}^{l(j)} \delta c_{i-1}^{(j)} + \beta_{i-1}^{l(j)} + \gamma_{i-1}^{l(j)} \delta v_{ph}, \quad 1 \le i \le N_2,\ j = A, B\,.$$

Coefficients $\alpha_i^{s(A)}$, $\beta_i^{s(A)}$, $\gamma_i^{s(A)}$, $i = -N_1, \ldots, 0$, $\alpha_i^{(j)}$, $\beta_i^{(j)}$, $\gamma_i^{(j)}$, $i = 0, \ldots, N_2$, $j = A, B$ can be easily calculated by the forward and backward elimination, respectively. Thus the problem is reduced to the system of five equations at the solid/liquid interface with respect to unknowns $(\delta c_0^{s(A)}, \delta c_0^{s(B)}, \delta v_{ph}, \delta c_0^{(A)}, \delta c_0^{(B)})^T$. Its solution is obtained directly by matrix inversion. The back substitution part of the method gives $\delta c_i^{s(j)}$, $i = -N_1, \ldots, 0$, $\delta c_i^{l(j)}$, $i = 0, \ldots, N_2$, $j = A, B$. The Gauss elimination is stable while the Jacobian appears to be a diagonally dominant matrix.

The solution *algorithm* can be summarized as follows:

1. Calculation of the Jacobian by using the latest solution $c^{s(A)}$, $c^{s(B)}$, v_{ph}, $c^{(A)}$, $c^{(B)}$ as a starting estimate for $\hat{c}^{s(A)}$, $\hat{c}^{s(B)}$, $\hat{v}_{ph}$, $\hat{c}^{(A)}$, $\hat{c}^{(B)}$.
2. Determination of coefficients α_i^s, β_i^s, γ_i^s, $i = -N_1, \ldots, 0$, $\alpha_i^{l(j)}$, $\beta_i^{l(j)}$, $\gamma_i^{l(j)}$, $i = 0, \ldots, N_2$, $j = A, B$ and reduction to the liquid/solid interface.
3. Direct matrix inversion for obtaining $\delta c_0^{s(A)}$, $\delta c_0^{s(B)}$, δv_{ph}, $\delta c_0^{(A)}$, $\delta c_0^{(B)}$.
4. Computing of the unknown functions l^s, l^l, φ_t and composition distribution in the solid and liquid phases at the next Newton's iteration.
5. Estimation of the convergence.
6. Advance to the next time step.

4. Numerical Results and Discussion

In this section the proposed fully implicit coupled algorithm was compared with a semi-implicit one, where the concentration distribution and interface location are determined consequently [1]. This technique treats l^s, l^l, v_{ph} in approximation of (3.1) – (3.3) in explicit way. Additional transport terms are approximated by the upwind scheme. Coefficients depending on interface rate v_{ph} are updated after determination of the concentration distribution in the bulk phase.

The equations obtained from the finite difference approximation are nonlinear only at the solid/liquid interface. As before the Thomas procedure is applied for the solution of the liner equations, but this time it is used with respect to unknown concentrations themselves [1, 13]. So we assume that:

$$\begin{aligned} \hat{c}_i^{s(A)} &= \sigma_{i+1}^s \hat{c}_{i+1}^{s(A)} + \eta_{i+1}^s, \quad -N_1 \le i \le -1\,, \\ \hat{c}_i^{l(j)} &= \sigma_{i-1}^{l(j)} \hat{c}_{i-1}^{l(j)} + \eta_{i-1}^{l(j)}, \quad 1 \le i \le N_2, j = A, B\,. \end{aligned} \tag{4.1}$$

Representation (4.1) allows us to reduce the system of governing equations to the set of four nonlinear equations at the solid/liquid interface with respect to unknowns $\hat{c}_0^{s(A)}$, $\hat{c}_0^{s(B)}$, $\hat{c}_0^{(A)}$, $\hat{c}_0^{(B)}$. They are determined by the Newton iteration [14]. Composition distribution in the bulk phases is obtained according to (4.1), then interface rate v_{ph} is calculated. In semi-implicit technique the Newton algorithm is applied only at the phase transition interface.

Both algorithms are used for the numerical study of liquid phase epitaxy of ternary alloys. The computer simulations are done for real phase diagram and experimentally used growth conditions [3, 5]. Diffusion coefficients are

$$D^{s(A)} = 5 \cdot 10^{-12} \frac{cm^2}{s}, \quad D^{l(A/B)} = 5 \cdot 10^{-5} \frac{cm^2}{s}.$$

The time step was taken $\tau = 0.5$ second. It is two hundred times larger than the one determined by the stability condition of explicit algorithms: $\tau \leq h^2/(2D^l) \approx 0.002s$.

Uniform but different space steps are used in solid and liquid phases. The number of grid points in the solid is $N_1 = 5000$ and in the liquid is $N_2 = 500$. The grid is sufficiently fine and allows us to predict accurately thin boundary layers in the vicinity of interface as well as to diminish numerical diffusion involved by the upwind approximation of transport terms in (3.1) – (3.3). The number of grid points and consequently the computational time can be decreased if non-uniform grids have been used. But it is not very important in the frame of this study, since our main objective is to reveal the advantage of the fully implicit conservative scheme.

Let us consider the following growth mode. Undersaturated $A - B - C$ solution at temperature T_0 is brought into contact with $A_xB_{1-x}C$ substrate. The composition of the liquid phase is in equilibrium with the solid phase $A_xB_{1-x}C$ at temperature $T_1 < T_0$. The growth is initiated by the programmed cooling: $T = T_0 - \alpha\, t$. At the early stage of the process the substrate, playing the role of material source, dissolves and feeds the solution with components A and B. Two processes contribute to the saturation of the liquid phase: substrate dissolution and cooling of the system. As soon as the solution at the vicinity of the interface becomes slightly supersaturated the process changes its direction from dissolution to growth.

This process was simulated by both methods. Fig. 3 demonstrates yielded composition distribution of AC in the solid phase. It is evident that the results provided by both algorithms are practically identical. It should be noted that attempts to implement the central difference approximation of transport terms in semi-implicit algorithm failed. Even on very fine time grids we have observed the substrate dissolution modelling growth regimes that should proceed without it.

But for another growth model the semi-implicit algorithm does not provide physically approved results. For instance, undersaturated solution is brought into contact with AC substrate instead of $A_xB_{1-x}C$. All the other parameters are the same as in the previous run. This time at dissolution stage the liquid

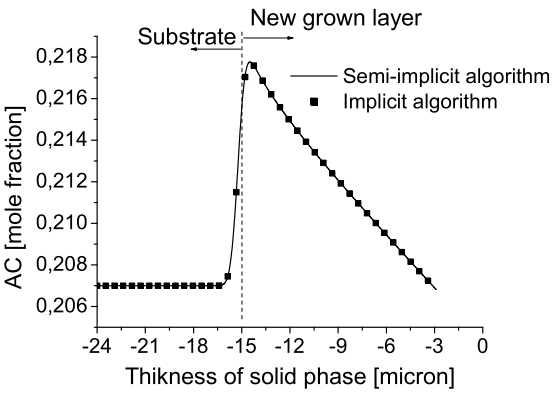

Figure 3. Composition distribution of AC in the solid phase.

phase is enriched only with component A, while component B diffuses from the liquid phase into the substrate. Thus, in the liquid phase, in vicinity of the interface concentration of component A increases, while concentration of component B decreases. The evolution of the liquid phase composition is shown on phase diagram of the system (Fig. 4). In the picture, the solid lines are the isotherms corresponding to T_0, T_1, the dashed ones are the lines of constant solid composition x. Sections of both curves give the composition x of a solid which is in equilibrium with a fluid of composition $x^{(A)}, x^{(B)}$ at a certain temperature. Thick line shows the calculated composition of the liquid phase at the interface in the considering growth mode. Point 1 denotes the initial composition of the liquid phase, point 2 is the equilibrium composition which immediately sets up at the interface when undersaturated solution is brought into contact with the substrate. Point 3 is the final composition of the liquid phase.

For the fully implicit coupled algorithm a transition of solution concentration at the interface is given in Fig. 4*a*. Due to dissolution of AC substrate concentration of component A in the liquid phase at the interface increases, while the solution becomes depleted with respect to component B.

In Fig. 4*b* for the semi-implicit scheme, we see that at the initial stage of the processes concentration of component B increases at the interface as if there is an artificial source of component B. This result is not physically valid, though the Newton method at the interface converges. The behavior of the solution does not improve if the time step is decreased.

The proposed fully implicit coupled algorithm allows us to perform full scale simulations for LPE process. Fig. 5 illustrates the early stage of the substrate dissolution. In the vicinity of liquid/solid interface concentration of component A gradually increases (Fig. 5b). At the same time component B diffuses into the solid phase producing a very thin boundary layer in the

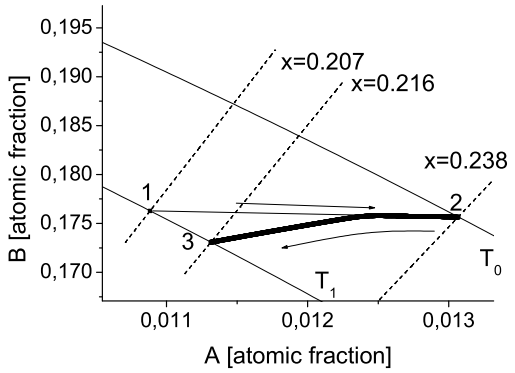

a) Implicit algorithm.

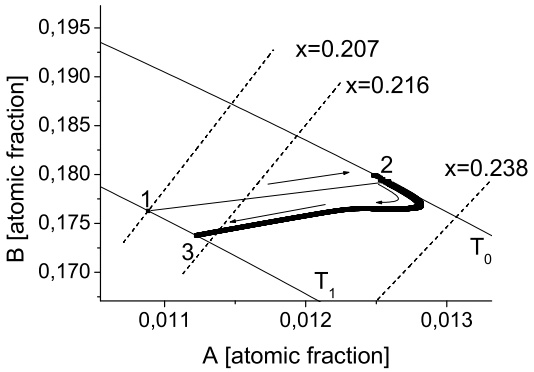

b) Semi-implicit algorithm.

Figure 4. Evolution of liquid phase composition at the phase transition interface during growth process.

solid phase. This process equilibrate the substrate, that is two component in the bulk, and ternary liquid phase (Fig. 5c, 5d). For the application, it is important to emphasize, that implicit algorithm does not require any additional adjustment of initial composition of liquid and solid phases for the convergence of iterations.

5. Conclusions

New numerical procedure is proposed for studying 1D self-consistent mathematical model of phase transition processes in ternary alloys. It is based on coupled solution of governing equations with respect to all unknown quantities. In fully implicit procedure the time step is chosen from accuracy considerations and is not dictated by stability demands. Variation of time steps from

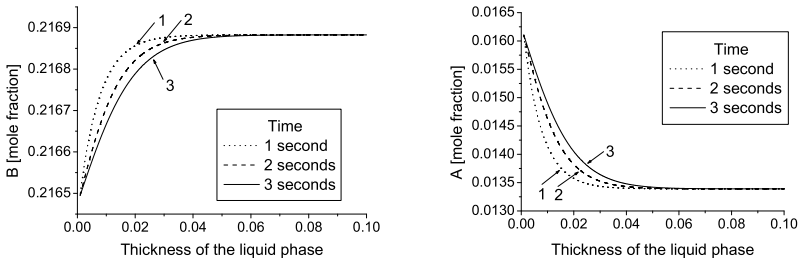

a) Distribution of B in the liquid phase b) distribution of A in the liquid phase

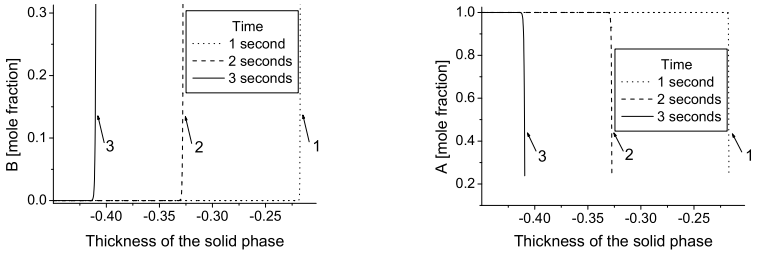

c) distribution of B in the solid phase d) distribution of A in the solid phase

Figure 5. Composition distribution in the vicinity of solid/liquid interface at the early stage of LPE process. Implicit algorithm.

0.001 second to 1 second does not influence on the quality of the solution. Also fully implicit algorithm does not require any preliminary adjustment of initial data as it usually happens in simulation of phase transition in multicomponent systems [10, 11].

The feasibility of the method is confirmed by numerical study of liquid phase epitaxy of ternary compounds. The simulations has been done for real phase diagram and practically used growth conditions.

References

[1] O.V. Chtcheritsa, O.S. Mazhorova and Yu.P. Popov. *Diffusive models for crystallization of multicomponent solutions.* The Keldysh Institute of Applied Mathematics, Preprint 24, Moscow, 2003. (in Russian)

[2] I. Crossley and M.B. Small. The physical processes occurring during liquid epitaxial growth. *Journal of Crystal Growth*, **27**(1), 35 – 48, 1974.

[3] I. A. Denisov, O. S. Mazhorova, Yu. P. Popov and N. A. Smirnova. Numerical modelling for convection in growth/dissolution of solid solution $Cd_xHg_{1-x}Te$ by liquid-phase epitaxy. *Journal of Crystal Growth*, **269**(2), 284 – 291, 2004.

[4] I.A. Denisov, V.M. Lakeenkov, O.S. Mazhorova and Yu.P. Popov. *Mathematical modelling for liquid phase epitaxy of $Cd_xHg_{1-x}Te$ solid solution.* The Keldysh Institute of Applied Mathematics, Preprint 65, Moscow, 1992. (in Russian)

[5] I.A. Denisov, V.M. Lakeenkov, O.S. Mazhorova and Yu.P. Popov. Numerical study for liquid phase epitaxy of $Cd_xHg_{1-x}Te$ solid solution. *Journal of Crystal Growth*, **245**(1), 21 – 30, 2002.

[6] L.A. Dmitrieva, O.S. Mazhorova, Yu.P. Popov, E.A. Tvirova and A.A.Shlenskii. *Mathematical Modelling. Production of Bulk Crystals and Semiconductor Structures. Computer simulation for solutal convection in liquid phase epitaxial growth of semiconductor materials.* Nauka, Moscow, 1986. (in Russian)

[7] S.V. Ermakov, O.S. Mazhorova and Yu.P. Popov. Mathematical modelling of electrophoretic separation of bio mixtures. Part 1. *Differential equations*, **28**(10), 1810 – 1821, 1992.

[8] S.V. Ermakov, O.S. Mazhorova and Yu.P. Popov. Mathematical modelling of electrophoretic separation of bio mixtures. Part 2. *Differential equations*, **28**(12), 2129 – 2137, 1992.

[9] K. Fletcher. *Computational techniques for fluid dynamics. V.1., V.2.* Mir, Moscow, 1991. (in Russian)

[10] M. Kimura, S. Dost, H. Udono, A. Tanaka, T. Sukegawa and Z. Qin. A numerical analysis for the conversion phenomenon of $GaAs$ to $GaAsP$ on a GaP substrate in an lpe system. *Journal of Crystal Growth*, **169**(1), 697 – 703, 1996.

[11] M. Kimura, Z. Qin and S. Dost. A solid – liquid diffusion model for growth and dissolution of ternary alloys by liquid phase epitaxy. *Journal of Crystal Growth*, **158**(1), 231 – 240, 1996.

[12] G. Müller and J. Friedrich. Challenges in modeling of bulk crystal growth. *Journal of Crystal Growth*, **266**(1), 1 – 19, 2004.

[13] A.A. Samarskii and E.S. Nikolaev. *Methods for the solution of grid equations.* Nauka, Moscow, 1978. (in Russian)

[14] A.A. Samarskii and Yu.P. Popov. *Finite difference schemes for the solution of gas dynamics problems.* Nauka, Moscow, 1992. (in Russian)

[15] A.A. Samarskii and P.N. Vabishchevich. *Computational Heat Transfer. Mathematical Modelling. Vol.1., Vol.2.* J. Wiley Sons, 1995.

[16] H.R. Vydyanath. Status of Te – rich and Hg – rich liquid phase epitaxial technologies for growth of $(Hg,Cd)Te$ alloys. *Journal of Electronic Materials*, **24**(9), 1275 – 1285, 1995.

Neišreikštinis skaitinis algoritmas fazės pernešimo uždaviniams daugiakomponenčiuose lydiniuose

O.V. Chtcheritsa, O.S. Mazhorova, Yu.F. Popov

Pasiūlytas naujas baigtinių skirtumų metodas fazės pernešimo daugiakomponenčiuose lydiniuose skaitiniam sprendiniui rasti. Algoritmas pagrįstas pilnai konservatyviąja baigtinių skirtumų schema ir vienalaikiu koncentracijos pasiskirstymo apibrėžimu kietoje ir skystoje fazėse, kaip ir sąlyčio paviršiuje. Skaitinis metodas yra besąlygiškai stabilus. Jis palygintas su kitais bendraisiais metodais, kurie nuosekliai apibrėžia koncentracijos pasiskirstymą ir sąlyčio paviršiaus padėtį.